# Density, Viscosity, Ionic Conductivity, and Self-Diffusion Coefficient of Organic Liquid Electrolytes: Part I. Propylene Carbonate + Li, Na, Mg and Ca Cation Salts

**Shiro Seki,[1,*,z] Kikuko Hayamizu,[2] Seiji Tsuzuki,[3,z] Keitaro Takahashi,[1] Yuki Ishino,[1] Masaki Kato,[1] Erika Nozaki,[4] Hikari Watanabe,[4] and Yasuhiro Umebayashi[4]**

[1]*Department of Environmental Chemistry and Chemical Engineering, School of Advanced Engineering, Kogakuin University, Hachioji-shi, Tokyo 192-0015, Japan*
[2]*Institute of Applied Physics, University of Tsukuba, Tsukuba, Ibaraki 305-8573, Japan*
[3]*National Institute of Advanced Industrial Science and Technology (AIST), Tsukuba, Ibaraki 305-8568, Japan*
[4]*Graduate School of Science and Technology, Niigata University, Nishi-ku, Niigata 950-2181, Japan*

To investigate physicochemical relationships between ionic radii, valence number and cationic metal species in electrolyte solutions, propylene carbonate with $Li[N(SO_2CF_3)_2]$, $Na[N(SO_2CF_3)_2]$, $Mg[N(SO_2CF_3)_2]_2$ and $Ca[N(SO_2CF_3)_2]_2$ were prepared. The temperature dependence of density, viscosity, ionic conductivity (AC impedance method) and self-diffusion coefficient (pulsed-gradient spin-echo nuclear magnetic resonance) was measured. The effects of cationic radii and cation valence number on the fluidity and transport properites (conductivity and self-diffusion coefficient) were analyzed.
 [DOI: 10.1149/2.0081803jes]

Manuscript submitted December 18, 2017; revised manuscript received January 23, 2018. Published February 23, 2018.

Research and development of lithium-ion batteries (LIBs) have focused on the efficient use of energy. Application fields of LIBs are spreading from portable commercial use (mobile phone and laptop PC) to large-scale energy systems (electric vehicle and accumulator for household use).[1] Furthermore, the usages (utilities, needs, requirements and demands) of industrial-scaled electricity storage systems using LIBs are increasing for applications alongside renewable energy systems (photovoltaics and/or wind energy) and frequency regulation demands. However, resources and stock amounts of Li are limited. Another reactive cationic species, such as high Clarke number $Na^+$ (2.63, 6th) and divalent cations $Mg^{2+}$ (1.93, 8th) and $Ca^{2+}$ (3.39, 5th) have been reported as new cationic species for next-generation batteries ($Li^+$: 0.0006, 27th).[2] The number of reports for battery operations using a Na (sodium) system is increasing, and they have focused on the research and development of electrode and electrolyte materials for, mainly, positive electrodes.[3–5] Because of the differences of ionic radii between $Li^+$ (60 pm) and $Na^+$ (95 pm), understanding the effects of ionic radii on electrolyte properties is important.[6,7] In addition, comparison between monovalent cations and divalent cations ($Mg^{2+}$: 65 pm,[8] $Ca^{2+}$: 99 pm[9]) is also important to understand the effects of valence number of cation on the electrolyte properties. In this study, an electrolyte solutions of propylene carbonate (PC) and $N(SO_2CF_3)_2^-$ ($[TFSA]^-$) anion-based metal (Li, Na, Mg and Ca) salts were prepared and evaluated by measuring their physicochemical properties. We investigate the dependence of static (density) and dynamic (macroscopic fluidity: viscosity, ionic mobility: ionic conductivity and microscopic ionic diffusivity: self-diffusion coefficient) properties of electrolytes on the cationic metal species of salts (ionic radii and valence number) and salt concentrations. We also analyze the intermolecular interactions of the cations with PC and $[TFSA]^-$ by ab initio molecular orbital calculations. Using the mearurements of static and dynamic properties and analysis of interactions, the expectations of innovative next-generation battery systems are discussed.

## Experimental

***Materials.***—PC (Kishida Chemical, battery grade) and metal cation salts (Table I) were used as the solvent and dissolved salts for electrolyte solutions, respectively. These materials were stored in a dry-argon-filled glove box. Amounts of PC and salts were weighed and mixed in a sample bottle, which allow us to obtain a homogeneous liquid electrolyte (salt concentration = [number of moles of dissolved salt/[mass of solvent]).

***Measurements.***—Density ($\rho$ / $gcm^{-3}$) and viscosity ($\eta$/mPas) were measured using a thermoregulated Stabinger-type viscosity and density/specific gravity meter ((Anton Paar, SVM3000G2, accuracy: $5 \times 10^2$ g $m^{-3}$). The measurements were performed during cooling from 353.15 to 283.15 K at 5 K intervals with an airtight stopper to avoid moisture and air contamination. The samples were thermally equilibrated at each temperature for at least 15 min prior to the measurement.

The ionic conductivity ($\sigma$) was measured on [stainless steel (SUS)/electrolyte solution sample/SUS] hermetically sealed cells and determined by the complex impedance method using an AC impedance analyzer (Bio-Logic VSP, 200 kHz - 50 mHz; impressed voltage: 10 mV) at temperatures between 353.15 and 283.15 K at 10 K intervals while cooling the samples in a thermoregulated incubator (ESPEC, SU-262). The samples were thermally equilibrated at each temperature for at least 90 min prior to the measurement.

The self-diffusion coefficient ($D$) was measured by a pulsed-gradient spin-echo nuclear magnetic resonance (PGSE-NMR) method using a Tecmag Apollo-NTNMR and a wide-bore 6.4 T SCM equipped with a JEOL pulsed-field gradient multiprobe. The samples were inserted into a 5 mm (outer diameter) NMR microtube (BMS-005J, Shigemi). The spectra of the solvent (PC), lithium cation and various anions were measured using $^1H$, $^7Li$ and $^{19}F$ atoms at frequencies of 270.2, 105.0 and 254.2 MHz, respectively. The attenuation of the echo signal $E$ was obtained by varying the duration $\delta$ of the pulsed-field gradient multiprobe at a fixed amplitude $g$. $D$ was determined by the regression of the Stejskal-Tanner equation[10]

$$E = \exp\left[-\gamma^2\delta^2 g^2 D\left(\Delta - \frac{\delta}{3}\right)\right] \quad [1]$$

**Table I. Measurement samples for electrolyte salts investigated in this study.**

| Code | Salt | Abbreviation | Suppliers | Purity |
|---|---|---|---|---|
| **A** | $Li[N(SO_2CF_3)_2]$ | LiTFSA | Kishida Chemical | > 99.9% |
| **B** | $Na[N(SO_2CF_3)_2]$ | NaTFSA | Kishida Chemical | > 98.0% |
| **C** | $Mg_{0.5}[N(SO_2CF_3)_2]$ | $Mg_{0.5}$TFSA | Kishida Chemical | > 99.0% |
| **D** | $Ca_{0.5}[N(SO_2CF_3)_2]$ | $Ca_{0.5}$TFSA | Kishida Chemical | > 99.0% |

*Electrochemical Society Member.
[z]E-mail: shiro-seki@cc.kogakuin.ac.jp; s.tsuzuki@aist.go.jp

onto the attenuation data, where γ is the gyromagnetic ratio of the observed nuclei and Δ is the interval between diffusion measurements. $D$ is independent of Δ for the homogeneous samples, as implied by Eq. 1. The measurements were performed at temperatures between 353.15 and 283.15 K while cooling with thermal equilibration at each temperature for 30 min prior to the measurement.

***Computational methods.***—The Gaussian 09 program[11] was used for the ab initio molecular orbital calculations with the basis sets implemented in the Gaussian program. The geometries of the complexes were fully optimized at the MP2/6-311G** level.[12] The intermolecular interaction energies ($E_{int}$) were calculated at the MP2/6-311G** level by the supermolecule method using the optimized geometries. The basis set superposition error (BSSE)[13] was corrected for all the interaction energy calculations using the counterpoise method.[14] Our previous calculations of the [emim][$BF_4$] and Li[TFSA] complexes[15] show that the basis set effects on the calculated interaction energies of the complexes are very small if basis sets including polarization functions are used and that the effects of electron correlation beyond MP2 are negligible. Therefore, we calculated the interaction energies of the complexes at the MP2/6-311G** level in this work. The stabilization energy for forming a complex from the isolated species ($E_{form}$) was calculated as the sum of the $E_{int}$ and the deformation energy ($E_{def}$), which is the sum of the increase in energy due to the deformation of the PC or $[TFSA]^-$ anion during formation of the complex.[16] Here, the $E_{def}$ was calculated at the MP2/6-311G** level. The electrostatic and induction energies were calculated using ORIENT version 3.2.[17] The electrostatic energy of the complex was calculated as interactions between distributed multipoles of the molecules. Distributed multipoles[18] up to the hexadecapole on all atoms were obtained from the MP2/6-311G** wave functions of an isolated molecule using the GDMA program.[19] The induction energy was calculated as interactions of polarizable sites with the electric field produced by the distributed multipoles of monomers.[20] The atomic polarizabilities of carbon (α = 10 au), nitrogen (α = 8 au), oxygen (α = 6 au), fluorine (α = 3 au) and sulfur (α = 20 au) were used for the calculations.[21] Distributed multipoles were used only to estimate the electrostatic and induction energies.

## Results and Discussion

***Static properties.***—To investigate the relationships between the physicochemical properties and dissolved cation species, the temperature dependences of various physicochemical parameters were measured. Figure 1a shows the temperature dependence of the ρ for electrolyte solutions of PC and metal-containing TFSA salts at 0.5 and 1.0 mol $kg^{-1}$. Highly linear relationships ($R > 0.999$) with temperature were obtained for all samples in the temperature range examined in this study, and the inclination of the calculated straight line was almost similar in all electrolyte systems. The measured ρ monotonically increased in the order Li[TFSA] < Na[TFSA] < $Mg[TFSA]_2$ < $Ca[TFSA]_2$ at all temperatures with the atomic weight of cationic metals. Figure 1b shows the salt concentration dependence of the ρ at 303.15 K for electrolyte solutions of PC and metal-containing TFSA salts. The ρ showed slightly convex upward tendency with salt concentration, and the deviation of the above-mentioned order was not confirmed. Furthermore, a divalent cationic salt system standardizes a subscript by the TFSA concentration as 0.5, and also this standardization was useful for the comparison of between monovalent and divalent cation salts to normalize the amounts of total ions.

***Transport properties.***—Figure 2a shows the temperature dependences of the η for electrolyte solutions of PC and metal-containing TFSA salts at 0.5 and 1.0 mol $kg^{-1}$ as Arrhenius-type plots. The obtained η increased in the order Li[TFSA] < Na[TFSA] < $Mg[TFSA]_2$ < $Ca[TFSA]_2$ at all temperatures. The η of electrolyte solutions was monovalent < divalent systems. This tendency appeared prominently in high salt concentrations, such as over 1.0 mol $kg^{-1}$. Figure 2b shows the salt concentration dependence of η at 303.15 K for

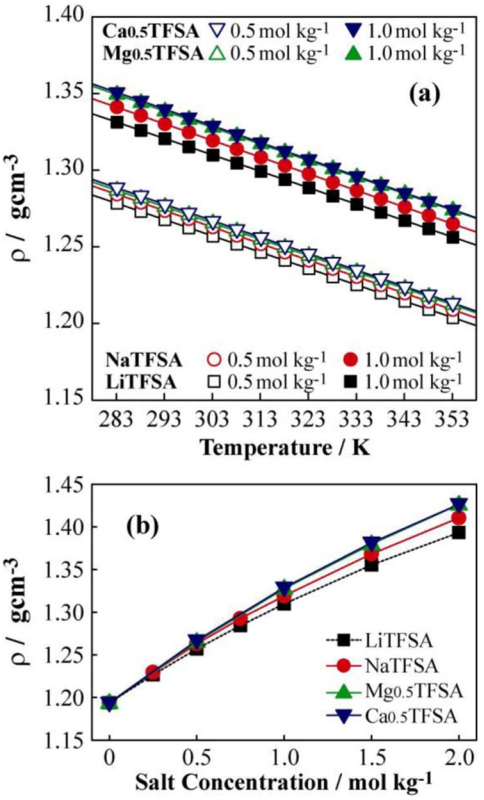


**Figure 1.** Temperature dependence (a), and salt concentration dependence of density at 303.15 K (b) for electrolyte solutions containing propylene carbonate and various TFSA salts.

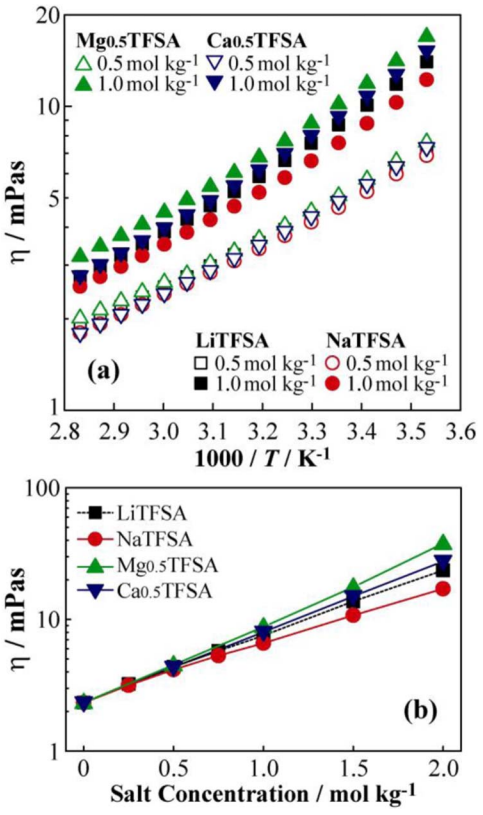


**Figure 2.** Temperature dependence (a), and salt concentration dependence of viscosity at 303.15 K (b) for electrolyte solutions containing propylene carbonate and various TFSA salts.

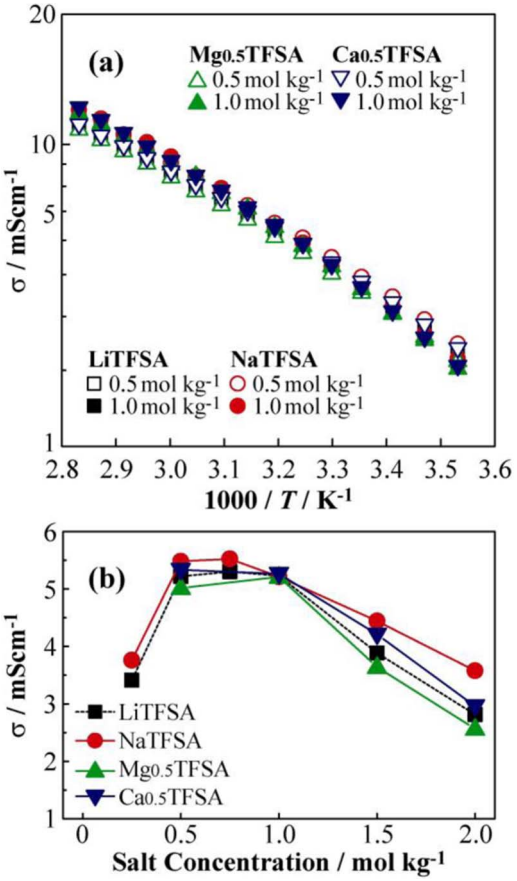


**Figure 3.** Temperature dependence (a), and salt concentration dependence of ionic conductivity at 303.15 K (b) for electrolyte solutions containing propylene carbonate and various TFSA salts.

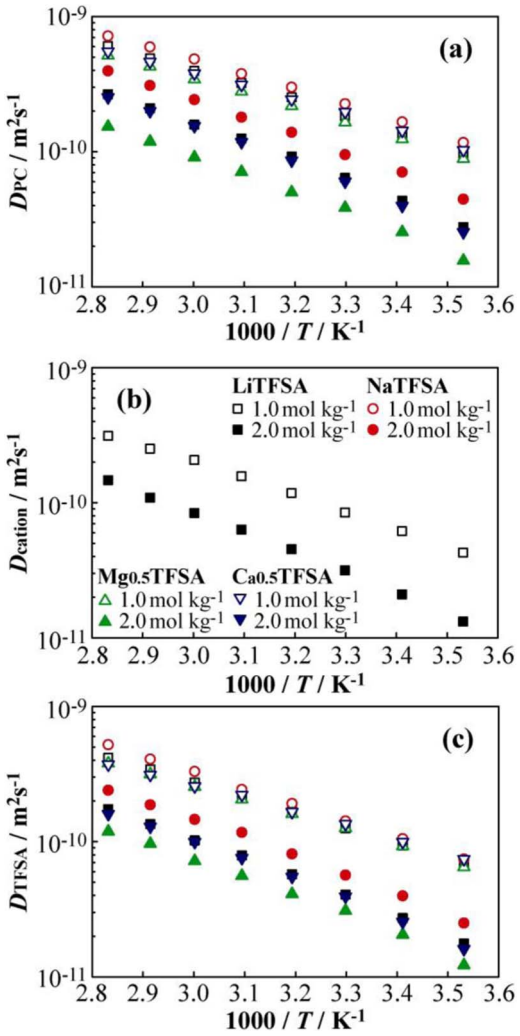


**Figure 4.** Temperature dependence of the self-diffusion coefficient for electrolyte solutions containing propylene carbonate and various TFSA salts (a: propylene carbonate, b: cation, c: TFSA anion).

electrolyte solutions of PC and metal-containing TFSA salts. The observed η indicates the tendency of the logarithmic increase with the increase in salt concentration, and the regression analysis of the calculated straight line was high ($R > 0.998$). Calculated ratios of the gradient of the straight line for LiTFSA: NaTFSA: $Mg_{0.5}$TFSA: $Ca_{0.5}$TFSA = 1: 0.85: 1.20: 1.07. In this study, the molar ratio of PC and metal cation salt was always approximately 10: 1, in the case of 1.0 mol $kg^{-1}$. The free solvent species unsolvated with metal cation should decrease with the increase in salt concentration, and this decrease of free solvent should significantly increase the η of the electrolyte solutions.

Figure 3a shows the temperature dependences of the σ for electrolyte solutions of PC and metal-containing TFSA salts at 0.5 and 1.0 mol $kg^{-1}$ as Arrhenius-type plots. The obtained σ indicates similar values for all the salt systems, which is different from that of the η results. Generally, σ in a unit volume is defined as

$$\sigma = \sum_j n_j q_j \mu_j, \qquad [2]$$

where $n$, $q$ and μ are the number, charge and mobility of the carrier ions in the specific volume, respectively. The suffix $j$ corresponds to the metal cation and TFSA anion. In this case, i.e., $q = 1$ ($Li^+$ and $Na^+$ cation and $[TFSA]^-$ anion) or 2 ($Mg^{2+}$ cation and $Ca^{2+}$ cation), σ values should depend on $n$ (related to the carrier density and ionic dissociation) and μ (related to the viscosity and ionic diffusion constants). Figure 3b shows the salt concentration dependence of σ at 303.15 K for electrolyte solutions of PC and metal-containing TFSA salts. The local maximum of the σ were observed for a salt concentration between 0.5 and 1.0 mol $kg^{-1}$ in all electrolyte systems. Moreover, the Na[TFSA] system indicated the highest σ of all salt concentrations. The Na[TFSA] system showed the lowest η for all the salt systems (Figure 2), therefore, it achieved the highest σ.

***Diffusive properties and ionic state of electrolytes.***—Figure 4 shows the temperature dependences of the self-diffusion coefficients of the solvent ($D_{PC}$, a), cation ($D_{cation}$, lithium only, b) and anion ($D_{TFSA}$, c) for electrolyte solutions of PC and TFSA salts at 1.0 and 2.0 mol $kg^{-1}$ as Arrhenius-type plots. Because of the large quadrupolar constant of $^{23}Na$, $^{25}Mg$ and $^{43}Ca$ from the viewpoint of NMR measurements, $D_{cation}$ was obtained only from the LiTFSA system ($^7Li$: small quadrupolar constant and high sensitivity). $D$s of all diffusive species were decreased with the increase of salt concentrations,[22] and the order of the $D$s were $D_{PC} > D_{TFSA} > D_{cation}$ in all electrolyte systems. The smaller $D_{PC}(Li^+)$ than $D_{PC}(Na^+)$ may be related to larger solvation energy around cation. Moreover, temperature dependences of $D$ showed the same tendencies as those for η (inverse) and σ. The order of the $D$ depending on the salt species is close to that of η. Figure 5 shows the salt concentration dependence of the self-diffusion coefficient ($D_{PC}$ and $D_{TFSA}$) at 303.15 K for electrolyte solutions of PC and TFSA salts. Although $D$ showed a monotonically decreasing trend with increase in concentration, almost the same trends of $D_{PC}$ (solvent) and $D_{TFSA}$ (ions) were recorded. In the case of the same salt concentration, the order of $D$ of all diffusive species were Na[TFSA] > Li[TFSA] > $Ca[TFSA]_2$ > $Mg[TFSA]_2$, and this was the same trend

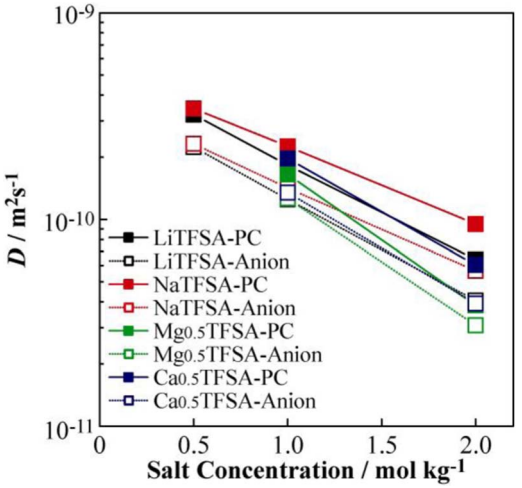


**Figure 5.** Salt concentration dependence of the self-diffusion coefficient at 303.15 K for electrolyte solutions of propylene carbonate and various TFSA salts.

as that of σ. Lager salt concentration dependence of *D* was observed in the solution of divalent metal cation salts compared with the solution of monovalent ones. Figure 6 shows the relationships between salt concentration and molar conductivity (Λ) at 303.15 K for electrolyte solutions of PC and TFSA salts. Although the difference of the absolute value for all Λ was very small, Λ increased with the enlargement of cation size for both the monovalent (Li[TFSA] < Na[TFSA]) and divalent ($Mg[TFSA]_2$ < $Ca[TFSA]_2$) cases. Moreover, the monovalent system indicated a little higher Λ than that of the divalent system. The Λ is controlled by the transport properties of electrolyte systems, if the molar concentration is the same. In this study, we measured the η, σ and *D* of the prepared electrolyte solutions and all the observed data were affected by μ, which is strongly related with valence number and size of the metal cation. Moreover, all the electrolyte systems showed a weak electrolyte-type dissociation behavior, which rapidly decreased Λ with the increase of salt concentration.

To analyze the correlations between the transport and ionic conduction properties, Figure 7a shows the relationships between (a) the inverse of viscosity (fluidity: $\eta^{-1}$) and ionic conductivity (σ) of

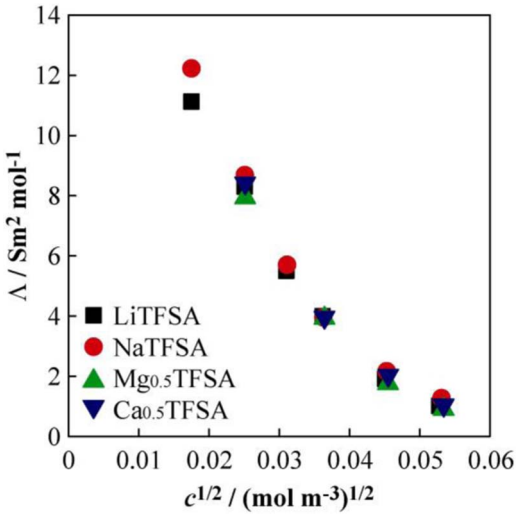


**Figure 6.** Relationships between salt concentration and molar conductivity at 301.15 K for electrolyte solutions of propylene carbonate and various TFSA salts.

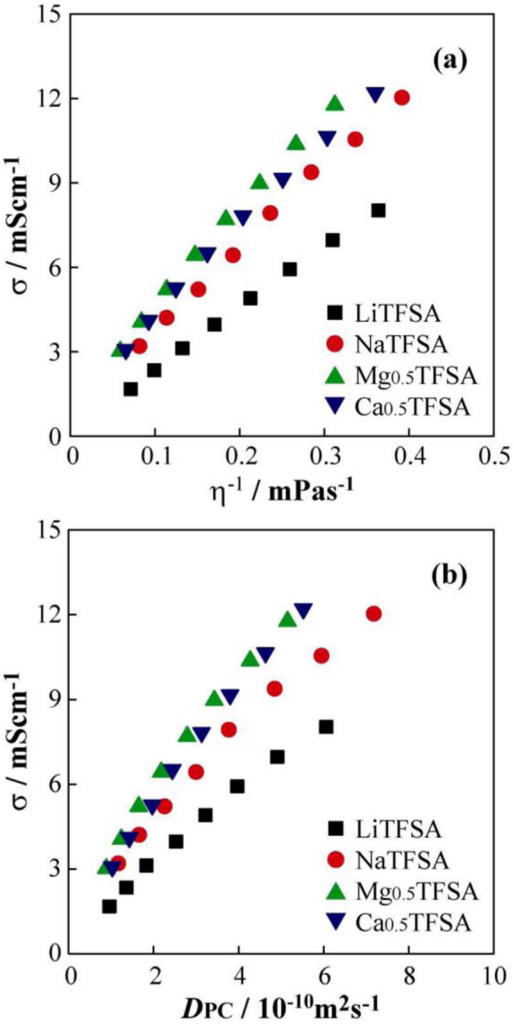


**Figure 7.** Relationships between (a) inverse of viscosity and ionic conductivity and (b) diffusion coefficient of propylene carbonate and ionic conductivity for electrolyte solutions of propylene carbonate and various TFSA salts.

the electrolytes, and the Figure 7b shows the relationship between self-diffusion coefficient of PC ($D_{PC}$) and σ for the electrolyte. The order of σ with both $\eta^{-1}$ and $D_{PC}$ were $Mg[TFSA]_2 \geqq Ca[TFSA]_2$ > Na[TFSA] > Li[TFSA]. The solution of divalent cation salts has higher ionic conductivity compared with the solution of monovalent cation salts when both solution has the same viscosity. This result is different from the tendency of anion changes.[23]

***Interactions of cations with PC and [TFSA]⁻ anion.***—The interactions of metal cations with PC and $[TFSA]^-$ anion were analyzed by ab initio molecular orbital calculations. The calculated stable structures for metal cation complexes with PC and $[TFSA]^-$ anion are shown in Figure S1. The stabilization energies by the formation of the complexes ($E_{form}$) were calculated for evaluating the metal cation dependence of the interaction energies. The calculated $E_{form}$ are summarized in Tables II and III. The $E_{form}$ depends strongly on the metal cation. The calculated $E_{form}$ for the complexes show that the attraction between the metal cations with PD and $[TFSA]^-$ anion increases in the order $Na^+ < Li^+ << Ca^{2+} < Mg^{2+}$. The order of the attraction coincides with the order of the viscosity and the reverse order of the self-diffusion coefficients of PC and ionic conductivity. This shows that the interactions of metal cations with PC and $[TFSA]^-$ anion play important roles in determining the transport properties of electrolytes. The strong attraction decreases the motion of ions (diffusion), which

**Table II. Stabilization energy calculated for metal cation complexes with propylene carbonate (PC) and contributions of electrostatic and induction interactions[a].**

| | $E_{form}$[b] | $E_{def}$[c] | $E_{es}$[d] | $E_{ind}$[e] | $E_{other}$[f] |
|---|---|---|---|---|---|
| $Li[PC]^+$ | −48.3 | 3.4 | −44.1 | −20.8 | 13.1 |
| $Na[PC]^+$ | −34.4 | 1.9 | −31.6 | −9.9 | 5.2 |
| $Mg[PC]^{2+}$ | −124.4 | 13.3 | −94.2 | −73.4 | 29.9 |
| $Ca[PC]^{2+}$ | −93.1 | 10.2 | −75.9 | −45.4 | 17.9 |

[a]Energy in kcal/mol. Geometries of complexes are shown in Figure S1.
[b]Stabilization energy by the formation of complex from isolated species. Sum of $E_{int}$ and $E_{def}$. The $E_{int}$ is the calculated interaction energy at the MP2/6-311G** level.
[c]The increase of energy of PC by the deformation of geometry associated with complex formation. See text.
[d]Electrostatic energy. See text.
[e]Induction energy. See text.
[f]$\Delta E_{other} = \Delta E_{int} - \Delta E_{es} - \Delta E_{ind}$. $\Delta E_{other}$ is mainly exchange-repulsion and dispersion energies.

**Table III. Stabilization energy calculated for metal cation complexes with $[TFSA]^-$ anion and contributions of electrostatic and induction interactions[a].**

| | $E_{form}$[b] | $E_{def}$[c] | $E_{es}$[d] | $E_{ind}$[e] | $E_{other}$[f] |
|---|---|---|---|---|---|
| Li[TFSA] | −136.5 | 5.9 | −139.5 | −47.8 | 44.9 |
| Na[TFSA] | −112.2 | 5.4 | −115.8 | −23.4 | 21.7 |
| $Mg[TFSA]^+$ | −318.4 | 25.7 | −281.7 | −183.4 | 120.9 |
| $Ca[TFSA]^+$ | −267.9 | 25.6 | −257.5 | −122.7 | 86.7 |

[a]Energy in kcal/mol. Geometries of complexes are shown in Figure S1.
[b]Stabilization energy by the formation of complex from isolated species. Sum of $E_{int}$ and $E_{def}$. The $E_{int}$ is the calculated interaction energy at the MP2/6-311G** level.
[c]The increase of energy of $[TFSA]^-$ by the deformation of geometry associated with complex formation. See text.
[d]Electrostatic energy. See text.
[e]Induction energy. See text.
[f]$\Delta E_{other} = \Delta E_{int} - \Delta E_{es} - \Delta E_{ind}$. $\Delta E_{other}$ is mainly exchange-repulsion and dispersion energies.

decreases the ionic conductivity and increases the viscosity of the electrolytes. The contributions of electrostatic and induction interactions to the attraction in the PC and $[TFSA]^-$ complexes are summarized in Tables II and III. The electrostatic interaction is the primary source of the attraction in the PC and $[TFSA]^-$ complexes. Although the contributions of induction interactions are smaller than those of electrostatic interactions, the contributions of induction interactions are not negligible. Especially magnitude of induction interactions is very large in the $Li^+$, $Mg^{2+}$ and $Ca^{2+}$ complexes. The strong electric field of small $Li^+$ cation and divalent $Mg^{2+}$ and $Ca^{2+}$ cations are the cause of the strong induction interactions.

In this study, we reported the measurement results and analysis of new cationic electrolyte solution including Na, Mg and Ca. There is a needed for new carrier ionic sources in next-generation batteries, and interfacial phenomena with electrodes are also important in battery technologies. We will report the analysis of electrode interfaces between electrolytes including new metal cationic salts/metallic electrodes from the viewpoint of application.

## Conclusions

Density, viscosity, ionic conductivity, and self-diffusion coefficient of PC + various cation salts (cation: Li, Na, Mg, Ca; anion: TFSA) salt were measured and analyzed systematically. Density was well correlated with molecular weight and valence of the metal salt. The inverse of viscosity (macroscopic fluidity), ionic conductivity and self-diffusion coefficient were increased with cationic sizes in both monovalent and divalent systems. These values of the monovalent cationic systems were larger than those of divalent ones.

## Acknowledgments

This work was partially supported by KAKENHI (24750192, 15K13767) from Japan Society for the Promotion of Sciences (JSPS).

## ORCID

Shiro Seki https://orcid.org/0000-0001-9717-2009
Kikuko Hayamizu https://orcid.org/0000-0003-3042-8289

## References

1. B. Dunn, H. Kamath, and J-M. Tarascon, *Science*, **334**, 928 (2011).
2. J. W. Choi and D. Aurbach, *Nat. Rev. Mater.*, **1**, 16013 (2016).
3. S-W. Kim, D-H. Seo, X. Ma, G. Ceder, and K. Kang, *Adv. Funct. Mater.*, **2**, 710 (2012).
4. M. D. Slater, D. Kim, E. Lee, and C. S. Johnson, *Adv. Funct. Mater.*, **23**, 947 (2013).
5. N. Yabuuchi, M. Kajiyama, J. Iwatate, H. Nishikawa, S. Hitomi, R. Okuyama, R. Usui, Y. Yamada, and S. Komaba, *Nat. Mater.*, **11**, 512 (2012).
6. K. Kuratani, N. Uemura, H. Senoh, H. T. Takeshita, and T. Kiyobayashi, *J. Power Sources*, **223**, 175 (2013).
7. K. Kuratani, I. Kishimoto, Y. Nishida, R. Kondo, H. T. Takeshita, H. Senoh, and T. Kiyobayashi, *J. Electrochem. Soc.*, **163**, H417 (2016).
8. H. Senoh, H. Sakaebe, H. Sano, M. Yao, K. Kuratani, N. Takeichi, and T. Kiyobayashi, *J. Electrochem. Soc.*, **161**, A1315 (2014).
9. S. Takeuchi, T. Fukutsuka, K. Miyazaki, and T. Abe, *Carbon*, **57**, 232 (2013).
10. E. O. Stejskal, *J. Phys. Chem.*, **43**, 3597 (1965).
11. Gaussian 09, Revision C.01, M. J. Frisch, G. W. Trucks, H. B. Schlegel, G. E. Scuseria, M. A. Robb, J. R. Cheeseman, G. Scalmani, V. Barone, B. Mennucci, G. A. Petersson, H. Nakatsuji, M. Caricato, X. Li, H. P. Hratchian, A. F. Izmaylov, J. Bloino, G. Zheng, J. L. Sonnenberg, M. Hada, M. Ehara, K. Toyota, R. Fukuda, J. Hasegawa, M. Ishida, T. Nakajima, Y. Honda, O. Kitao, H. Nakai, T. Vreven, J. A. Montgomery Jr., J. E. Peralta, F. Ogliaro, M. Bearpark, J. J. Heyd, E. Brothers, K. N. Kudin, V. N. Staroverov, R. Kobayashi, J. Normand, K. Raghavachari, A. Rendell, J. C. Burant, S. S. Iyengar, J. Tomasi, M. Cossi, N. Rega, J. M. Millam, M. Klene, J. E. Knox, J. B. Cross, V. Bakken, C. Adamo, J. Jaramillo, R. Gomperts, R. E. Stratmann, O. Yazyev, A. J. Austin, R. Cammi, C. Pomelli, J. W. Ochterski, R. L. Martin, K. Morokuma, V. G. Zakrzewski, G. A. Voth, P. Salvador, J. J. Dannenberg, S. Dapprich, A. D. Daniels, Ö. Farkas, J. B. Foresman, J. V. Ortiz, J. Cioslowski, and D. J. Fox, Gaussian, Inc., Wallingford CT, 2009.
12. C. Møller and M. S. Plesset, *Phys. Rev.*, **46**, 618 (1934). b) M. Head-Gordon, J. A. Pople, and M. J. Frisch, *Chem. Phys. Lett.*, **153**, 503 (1988).
13. B. J. Ransil, *J. Chem. Phys.*, **34**, 2109 (1961).
14. S. F. Boys and F. Bernardi, *Mol. Phys.*, **19**, 553 (1970).
15. S. Tsuzuki, H. Tokuda, K. Hayamizu, and M. Watanabe, *J. Phys. Chem. B*, **109**, 16474 (2005).
16. S. Tsuzuki, K. Hayamizu, S. Seki, Y. Ohno, Y. Kobayashi, and H. Miyashiro, *J. Phys. Chem. B*, **112**, 9914 (2008).
17. A. J. Stone, A. Dullweber, M. P. Hodges, P. L. A. Popelier, and D. J. Wales, *Orient: a program for studying interactions between molecules version 3.2*, University of Cambridge, 1995.
18. A. J. Stone, *The theory of intermolecular forces second edition*, Clarendon Press: Oxford, 2013. b) A. J. Stone and M. Alderton, *Mol. Phys.*, **56**, 1047 (1985).
19. A. J. Stone, *J. Chem. Theory Comput.*, **1**, 1128 (2005).
20. A. J. Stone, *Mol. Phys.*, **56**, 1065 (1985).
21. P. T. van Duijnen and M. Swart, *J. Phys. Chem. A*, **102**, 2399 (1998).
22. S. A. Krachkovskiy, J. D. Bazak, S. Fraser, I. C. Halalay, and G. R. Goward, *J. Electrochem. Soc.*, **164**, A912 (2017).
23. S. Seki, K. Hayamizu, S. Tsuzuki, K. Takahashi, Y. Ishino, M. Kato, E. Nozaki, N. Arai, H. Watanabe, and Y. Umebayashi, to be submitted.